HAND MOVEMENTS CLASSIFICATION FOR MYOELECTRIC CONTROL SYSTEM USING ADAPTIVE RESONANCE THEORY

H.Jahani Fariman*, Siti A. Ahmad, M. Hamiruce Marhaban, M. Alijan Ghasab, Paul H. Chappell

Department of Electrical & Electronic Engineering, Faculty of Engineering, University Putra Malaysia, 43400 Serdang, Selangor, Malaysia.

* Corresponding author email: ee.hessam.jahani@gmail.com , Tel: +60173936647

-H. Jahani Fariman, Siti A. Ahmad, M. Hamiruce Marhaban & M. Alijan Ghasab are with the Control System and Signal Processing Research Group, Department of Electrical & Electronic Engineering, Faculty of Engineering, University Putra Malaysia 43400 UPM Serdang, Selangor, Malaysia.

-Paul H. Chappell is with Electronics & Computer Science, University of Southampton, SO17 1BJ Highfield, UK.

ABSTRACT

This research proposes an exploratory study of a simple, accurate, and computationally efficient movement classification technique for prosthetic hand application. Surface myoelectric signals were acquired from the four muscles, namely, flexor carpi ulnaris, extensor carpi radialis, biceps brachii, and triceps brachii, of four normal-limb subjects. The signals were segmented, and the features were extracted with a new combined time-domain feature extraction method. Fuzzy C-means clustering method and scatter plot were used to evaluate the performance of the proposed multi-feature versus Hudgins' multi-feature. The movements were classified with a hybrid Adaptive Resonance Theory-based neural network. Comparative results indicate that the proposed hybrid classifier not only has good classification accuracy (89.09%) but also a significantly improved computation time.

KEYWORDS: Pattern Recognition; EMG; Adaptive Resonance Theory; Neural Network; prosthetic hand.

1. BACKGROUND:

The human hand is able to complete a complex range of sophisticated movements that enables us to interact with our environment and communicate with one another. The state of

the art prosthetic hand has been designed to fairly accurate the natural limb in both form and function[1]. Excluding cosmetic prosthetic hand, there is the functional type which is divided into two categories: body powered and externally powered. In a body-powered prosthesis, motion is transmitted to the prosthesis via a cable control system. For externally powered prosthesis, myoelectric control is the most employed method of control in commercially available bionic limbs. It relies on complex algorithms to make sense of the massive amount of electrical activity in the stump, which is affected by everything from movement in the shoulder or elbow to the heartbeat[2]. Considering upper limb prosthetic devices, the electromyography (EMG) signal is widely used as an input for the actuation of upper limb movements. In fact, the heart of myoelectric control is the fact that the primary source of control information for the system being controlled comes from the EMG signal. Myoelectric control is the technique of using signal processing to extract information from the EMG signal to determine the intended motion of a person and aid him or her in controlling an assisting device [3]. The typical approach to myoelectric control is to use a pattern recognition scheme [4]. This approach recognizes one of several predetermined classes. These classes represent certain motions such as elbow flexion and extension.

A block diagram representing a myoelectric pattern recognition prosthetic hand scheme is shown in Figure 1. The test subject ultimately controls the end device with their EMG signals. Prior to any pattern recognition analysis, the EMG data acquisition is accomplished using surface electrodes and a bioinstrumentation device. Included in the EMG data acquisition block is any data segmentation or windowing which involves dividing up the EMG signal into windows. It also includes any preprocessing techniques such as filtering. Many bioinstrumentation devices provide the necessary analog filtering for EMG applications. The core pattern recognition blocks are feature extraction and classification. EMG feature extraction is a very important step and can determine the efficiency and accuracy of the classifier.

Despite significant developments in the prosthetic hand industry in the last decade, commercial prosthetic hands with high accuracy remain expensive. Despite the massive research interest in myoelectric control systems (MCS), only a few studies have conducted quantitative comparisons of the performance and real-time efficiency of the method. The desired system should be able to efficiently perform the essential movements in terms of both movement classification accuracy and computational time. Considering essential hand movements, previous research, survey and assessment conducted from amputees [1, 5-7] and in reliable prosthetic devices such as the Southampton Hand[8] can be considered as a criterion. They should include flexion and extension of finger, wrist and elbow for doing routine chores. Here, the complex movements of grabbing can be excluded as the system we are headed to design should also be simple enough to deploy in a non-exclusive and inexpensive real-time implementation device, such as an embedded microcontroller. One potential solution is to investigate a simple, accurate, and computationally efficient classification of hand movements for MCS.

A considerable number of studies on soft computing techniques have been published, especially fuzzy logic systems and neural networks, for bio-signal classification in numerous biomedical applications [9-12] and expert systems for recognition [13]. Some EMG pattern-recognition applications have used linear discriminant analysis (LDA) or a similar Bayesian approach as parametric classification [13-18]. The k-Nearest Neighbor (k-NN) is another simple yet accurate non-parametric classifier that does not require training. Regarding MCS, Rasheed et al. [19] introduced an adaptive fuzzy k-NN classifier for EMG decomposition that significantly outperformed adaptive certainty classifiers. The same researchers also introduced another approach of using fuzzy and k-NN in [20] by developing a software program based on MATLAB, which can be used as a motor unit potential classifier. Kim et al. [21] compared k-NN with LDA and quadratic discriminant analysis (QDA) and concluded the significant classification improvement with k-NN. [22] did the same for EEG signals and found k-NN superiority.[23] proposed an exploratory analysis for the most robust classification among several features and classifiers. The result indicated that LDA is more robust than k-NN, QDA, support vector machine, and multilayer perceptron neural network.
With performance and simplicity in learning-based classification approaches both considered, among the efficient neural network-based supervised learning methods are adaptive resonance theory (ART) and ARTMAP, which is a modification of ART for supervised learning structure and was first discussed by Carpenter et al. [24]. Verzi et al. [25] proposed a new fuzzy ARTMAP neural network called hierarchical ARTMAP as a classification approach for a probabilistic setting, as well as compared the generalization capability result with Gaussian ARTMAP, old fuzzy ARTMAP, and boosted ARTMAP. Xu et al. [26, 27] proposed a Mahalanobis distance-based modification of the Gaussian ARTMAP network. Mahalanobis distance-based ARTMAP (MART) networks use the Mahalanobis distance for activation and matching functions and rely on the full covariance matrices of clusters rather than just their diagonal part. In the same character recognition tests referred to in the previous section, Xu determined that MART outperformed fuzzy ARTMAP and Gaussian ARTMAP by 3% to 6% in almost half the number of output nodes. Several ART-based approaches, including Hierarchical ARTMAP [25],Distance Based ARTMAP [26, 28], Distributed ARTMAP [29, 30], Fuzzy ARTMAP [30-32], ARTMAP-IC [32, 33] and ART-EMAP [34, 35] have been developed and used for object recognition in the last decade.

2. OBJECTIVE:

The current study intends to propose a pattern-recognition approach for the classification of hand movements in a manner in which the functionality and accuracy of a myoelectric prosthetic hand control system can be improved. Investigation and evaluation are first conducted on the feature extraction methods for the proposed simple and accurate multi-feature. An ensemble classification method of movements with the use of an ART-based neural network is then designed. The performance of the proposed classification method is evaluated and compared with those of other high-accuracy methods in terms of classification accuracy and computation time. Finally, a simple, accurate, and computationally efficient classification approach of hand movements for MCS is achieved (Figure 2).

3. MATERIALS AND METHODS

3.1. EMG data acquisitions

The datasets have been used in this research were acquired based on SENIAM protocol for EMG acquisition [36] for the same essential movements. The detailed information of acquisition has been summarized in Table 1.

3.1.1. Dataset 1: Evaluating redundancy of EMG features

The EMG data that were used for the first aim of this study were obtained from the University of Essex [37], particularly from two forearm muscle channels, namely, flexor carpi ulnaris (FCU) and extensor carpi radialis (ECR), as shown in Figure 3. One healthy subject was asked to perform five essential upper-limb movements, including wrist flexion/extension (movement 1), elbow flexion (movement 2), finger flexion/extension (movement 3), co-contraction (movement 4), and isometric contraction (movement 5), as shown in Figure 4.It should be mentioned that only these 5 movements can undertake the necessity of a prosthetic hand empowerment. While, the dataset not only consists of flexion/extension of finger, elbow and wrist; which based on previous survey are crucial prosthetic hand movements; it is also included co-contraction and isometric contraction that are two essential contractions[5, 38].

3.1.2. Dataset 2: Investigating optimal EMG multi-feature and classification

The EMG data that were used for the second aim were obtained from an approved experimental procedure in a previous MCS study in the School of Electronics and Computer Science of the University of Southampton [38]. Such a study was based on the SENIAM protocol on surface EMG acquisition [36]. The main data result from the 12 normal-limb subjects aged 20 to 30 years old consists of 1 trial of 5 essential movements' acquisition—wrist flexion/extension, finger flexion/extension, elbow flexion, co-contraction, and isometric contraction—from four muscles, namely, FCU, ECR, biceps brachii (BB), and triceps brachii (TB), with a speed of *60 beats per minute* controlled by a metronome, as shown in Figure 3.

3.2. Data Segmentation

The width of the analysis window is a critical parameter. The lower limit for the window width is restricted by the low statistical variance of the features extracted from small windows that yield low classification accuracy. The upper limit is given by the time required to acquire and process the signal to obtain the final decision. Englehart and Hudgins determined that the analysis windows of approximately 256 ms led to acceptable classification accuracy values and allowed the system to be more robust and responsive than the analysis windows with a short length [39]. Another approach on time segment optimization, which was conducted by Du and Vuskovic, indicated that increasing the segment length from 100 ms to 400 ms increases the classification accuracy to 20% [40]. Asghari and Hu used a similar approach [41], in which they proved that increasing the

segment length from 200 ms to 500 ms would lead to an upsurge in performance by 3%. In the current study, the EMG signals for each hand motion were partitioned into 400-point segments that corresponded to 265.6 ms of contraction.

Choosing the data windowing technique is important for data segmentation after the segment length is decided on. An overlapping technique was applied according to the literature and in consideration of real-time constraints, which are the concern of the current study and are discussed in [6]. In [41], overlapped segmentation was proven to make a controller four times faster without a noticeable degradation in accuracy. Figure 5 shows that the overlapping (increment) time should be greater than the processing time [6, 39] because the processor must have enough time to execute programs for the feature segment and generate a decision before the next segment arrives. Moreover, the processing time should often be less than 50 ms. The overlapping segment length in the current study is 200 points, which correspond to 132.5 ms.

3.3 Feature extraction methods description

As mentioned in the introduction, one of the primary aims of this study is to develop an accurate yet simple offline pattern recognition myoelectric classification scheme for a rehabilitation prosthetic hand. The selected classifier in a pattern recognition scheme can be argued to be of little importance if the extracted features are not clustered in feature space, that is, the success of classification depends more on the features extracted than on the classifier itself. Emphasis was placed on using features that provide a well-separated feature space, with focus on easy implementation and the use of a time-saving extraction method. The focus is time-domain features, as discussed in the literature review chapter; these features are primarily based on the statistical characteristics of signals. No transformation is included, so the implementation is easy.

An enormous amount of data is present in the 265 ms (400 points) EMG recordings. For a classifier to be computationally efficient, it must use an adequate method of feature extraction. This method quantifies large data sets into a few features that optimally distinguish that set of data from other sets and enable a classifier to group that data set with related data sets. Time-domain features were selected as the main feature extraction method in this study. Moreover, several modifications in the multi-feature have been made by addition of the mean frequency (MNF). A review of these features follows. Figure 6 shows that all five successive movements have been used. The descriptions of the feature methods were combined and used as a multi-feature.

Mean absolute value (MAV) first presented by Hudgins [42, 43]. It is defined as an average of the absolute value of all the EMG signal amplitude in a segment, formulated like this:

$$\mathrm{MAV} = \frac{1}{N}\sum_{i=1}^{N}|x_i| \qquad (1)$$

Waveform length (WL) is a scale shows how complex is the EMG signal [41, 42]. The feature is presented in a simple formulation as the cumulative length of the EMG waveform over the time segment:

$$WL = \sum_{i=1}^{N-1}|x_{i+1} - x_i| \qquad (2)$$

Zero crossing (ZC) is the time-domain definition of EMG segment frequency information [42].It counts the number of times the signal crosses zero. A threshold would be defined to avoid the natural noises and fluctuations caused by low-voltage. $ZC = \sum_{i=1}^{N-1} \left[\text{sgn}\left(x_i \times x_{i+1}\right) \cap \left|x_i - x_{i+1}\right| \right] \geq \text{threshold}$ (3)

$$\text{sgn}(x) = \begin{cases} 1, & \text{if } x \geq \text{threshold} \\ 0, & \text{otherwise} \end{cases} \quad (4)$$

Root mean square (RMS) is again a well-known feature analysis regarding EMG signal [21, 44]. It is also alike to the standard deviation method. The mathematical definition of RMS feature can be expressed as:

$$\text{RMS} = \sqrt{\frac{1}{N} \sum_{i=1}^{N} x_i^2} \quad (5)$$

Slope sign change (SSC) is linked to ZC and WAMP features [42, 45]. It is another method to represent frequency information of the EMG signal. It is a number of times that the slope of the EMG signal changes sign. For the same reason as ZC we defined a threshold here, too. The mathematical expression is:

$$SSC = \sum_{i=2}^{N-1} f[(x_i - x_{i-1}) \times (x_i - x_{i+1})] \quad (6)$$

$$f(x) = \begin{cases} 1, & if\ x\ \geq threshold \\ 0, & otherwise. \end{cases} \quad (7)$$

Mean Frequency (MNF) is an average frequency which is calculated as sum of the product of the EMG power spectrum and the frequency divided by the total sum of the spectrum intensity e.g. [41]. Central frequency (fc) and spectral center of gravity are other calling names of the MNF feature [40]. It can be calculated as

$$MNF = \sum_{j=1}^{M} f_j P_j \Big/ \sum_{j=1}^{M} P_j \quad (8)$$

where fj is frequency of the spectrum at frequency bin j, Pj is the EMG power spectrum at frequency binj, and M is length of the frequency bin.

The whole process of feature combination and selection depicts in Figure 7. It should be considered that the proposed feature extraction and evaluation in Figure 7 has been repeated in each round of cross-validation process to improve the reliable classification result and decrease error and bias.

3.4. Feature evaluation

As been shown in the Figure 6, the amplitude of the myoelectric signal fluctuated progressively and for this reason, the amplitude varied in the EMG segments. Moreover, each of feature extraction methods scales the EMG amplitude in a different value range. To overcome this inconsistency, the signal amplitude after feature extraction was normalized within a fixed range of [0, 1] in all channels (Figure 10, 11 and 12). It should be also considered that no transformation of features was done as the simplicity and computational efficiency is the priority in this research.

3.4.1. Dataset 1: Fuzzy C-mean clustering and scatter plot

Fuzzy c-means (FCM) is an iterative data clustering technique in which a dataset is grouped into n clusters with every data point in the dataset belonging to every cluster to a certain degree. This iteration is based on minimizing an objective function that represents the distance from any given data point to a cluster centre weighted by that data point's membership grade. In other words, FCM clusters the data based on their nature into the specified groups.

It starts with an initial guess for the cluster centers, and then FCM iteratively moves the cluster centers to the right location within a data. Formally, clustering an unlabeled data $X = \{x1, x2, \dots, xN\} c \subset R^h$, where N represents the number of data vectors and h the dimension of each data vector, is the assignment c of partition labels to the vectors in X. c-Partition of X constitutes sets of (c . N) membership values that can be conveniently arranged as a (c . N) matrix $U = [u_{ik}]$. The problem of fuzzy clustering is to find the optimum membership matrix U [46]. The result of FCM clustering would be shown in scatter plots for different feature sets.

Moreover, it should be considered that clustering and scatter plot both are used as a visual way of evaluating feature redundancy and so for a better and more accurate evaluation these features should be employed in a classification process and then the classification accuracy should be compared.

3.4.2. Dataset 2: Feature evaluation using Linear Discriminant Analysis

Considering further investigation on evaluating the proposed features, a well known easy implementing linear classifier-, LDA has been used. LDA is a classification method originally developed in 1936 by R. A. Fisher. It is simple, mathematically robust and often produces models whose accuracy is as good as more complex methods. LDA is based upon the concept of searching for a linear combination of variables (predictors) that best separates the two classes (targets). To capture the notion of separability, Fisher defined the following score function.

$$Z = \beta_1 x_1 + \beta_2 x_2 + \dots + \beta_d x_d \qquad (9)$$

$$S(\beta) = \frac{\beta^T \mu_1 - \beta^T \mu_2}{\beta^T C \beta} \qquad \text{Score function} \qquad (10)$$

$$S(\beta) = \frac{\bar{Z_1} - \bar{Z_2}}{Variance\ of\ Z\ within\ groups} \quad (11)$$

Given the score function, the problem is to estimate the linear coefficients that maximize the score, which can be solved by the following equations.

$$\beta = C^{-1}(\mu_1 - \mu_2) \quad \text{Model Coefficients} \quad (12)$$

$$C = \frac{1}{n_1+n_2}(n_1 C_1 + n_2 C_2) \quad \text{Pooled covariance matrix} \quad (13)$$

Where:

β: Linear Model coefficients

C_1, C_2: Covariance matrices

μ_1 , μ_2 : Mean vectors

The results of the LDA were performed by a 3-fold cross validation in each subject and the classification accuracy was computed as an average accuracy based on the results from cross validation testing of all subjects. It should also be considered that to illustrate the optimal feature extraction method, a comparison of the proposed multi-feature performance versus a number of the existing combinations of time domain features will be discussed. For this reason, two successful EMG feature sets were selected that are (1) Hudgins's feature set: MAV, WL, ZC, and SSC [42], and (2) Du's feature set: IEMG, VAR, WL ZC, SSC, and WAMP [47].

3.5. Classification

Classification is the most important stage that affects the final performance of the myoelectric pattern-recognition system. At this stage, the classifier should be able to learn the different muscle contraction patterns selected to actuate the prosthetic device. The ART neural network was selected over other techniques as the signal classifier because it can generalize complex data. The final model is also simple and accurate enough to meet the real-time constraints. Several ART-based approaches, including hierarchical ARTMAP [25], Distance Based ARTMAP [26, 48], Distributed ARTMAP [29, 30], Fuzzy ARTMAP (Carpenter et al. 1992, Llobet et al. 2002, Nachev et al. 2010), ARTMAP-IC [32, 33] and ART-EMAP [34, 35] were developed and used for object recognition in the past decade..

In this study, four ART-based classification techniques, namely, fuzzy ARTMAP, dARTMAP, ART-EMAP, and ARTMAP-IC, are employed as classifiers. A new hybrid classifier called Best-ART outperforms these four methods.

In order to calculate the performance of our approach, the whole EMG data is divided into training and test sets, and k-fold cross- validation is used subsequently. The training set is used to build a classification model and the test set is used to verify it. We choose k- fold cross-validation which is a well-known method for evaluation. k-Fold cross validation is used by numerous researchers to reduce the bias related with

random sampling of the training and test sets. In k-fold cross validation, the whole data set is randomly split into k mutually exclusive subsets (folds) of approximately equivalent size. The classification model is trained and tested k times. In other words, it is trained on all but one of the folds and tested on the remaining single fold. The cross-validation accuracy (CVA) is the average of the k individual accuracy measures where k (3 in this case) is the number of folds used. According to detailed information from [49] and considering the number of experiments, reducing computation time which is one of our goal in this research, also size of the dataset (not that sparse to increase number of folds or using leave-one-out), a repeated 3-fold cross validation has been used. It is almost the same method as 3-fold cross validation but we repeated it for 400 times, to decrease type-I error and obtain a more reliable performance.

3.5.1. Combined ART-based classification (Best-ART)

The rationale behind the growing interest in multiple classifier systems is the recognition that the classical approach in designing a pattern recognition system, which focuses on determining the best individual classifier, involves several serious drawbacks. The most common type of multiple classifier system includes an ensemble of classifiers and a function for the parallel combination of classifier outputs. However, a large number of methods to create and combine multiple classifiers were proposed in the last few years (Kim et al., 2011). From the ARTMAP-based classification architecture that has been reviewed in Section 2.5.4 of the literature review section, a MATLAB code has been developed to select the best technique among four ART-based classification techniques, namely, fuzzy ARTMAP, dARTMAP, ART-EMAP, and ARTMAP-IC. The ensemble algorithm is based on the classification accuracy percentage for each subject. An improvement is achieved by this coding approach, which consists of all four ARTMAP classifiers that select the best technique based on the classification accuracy for each subject of the data set. Training and classification with the use of the technique then continues. The maximum rule has been used as combination, which is one of the biased rules and has an effective computation time. This classification approach is abbreviated as Best-ART in the result and discussion sections. Figure 7 shows the entire process of the combined ART-based classifiers.
To test the feasibility of the ART network, the classification accuracy in the test set was first computed for the classifiers trained with the data from each recording session of the 12 subjects. Englehart et al. [50] found that a high classification accuracy does not guarantee good classifier performance and usability. Thus, other parameters, such as the computation time of the proposed algorithm, should be considered in evaluating classifier performance. To test the hypothesis that the ART classifier can accurately perform, the training time, classification time, and elapsed time of the proposed classifier are obtained, and a comparison is made between the ART method and k-NN and LDA as two efficient and common classification methods.

3.5.2.ARTMAP learning process

ARTMAP is often applied using the simplified version shown in Figure 8. It is obtained by combining an ART unsupervised neural network [48] with a map field and actually specialized for pattern classification approach. It consists of two fully related layers of nodes: A M node input layer F1 and a N node competitive layer F2. A set of real-valued weights $W = \{ w_{ij} \epsilon [0,1]: \ i = 1,2,\dots,M \ ; \ j = 1,2,\dots,N \ \}$ is associated with the F_1 to F_2 layer connections. Each F_2 node j represents a recognition category that learns a prototype vector $wj = (w_{1j} , w_{2j} , \dots , w_{Mj})$. The F_2 layer is connected through learning associative links to an L node map field F^{ab} , where L is the number of classes in the output space.

A set of binary weights $W^{ab} = \{ w^{ab}_{jk} \epsilon [0,1]: \ j = 1,2,\dots,N \ ; \ k = 1,2,\dots,L \}$ is associated with F_2 to F^{ab} connections. The vector $w_j^{ab} = (w_{j1}^{ab} , w_{j2}^{ab} , \dots , w_{jL}^{ab})$ links the F_2 node j to one of the L output classes. During training, ARTMAP classifiers perform supervised learning of the mapping between training set vectors $a = (a_1 , a_2 , \dots , a_m)$ and output labels $t = (t_1, t_2, \dots , t_L)$, where $t_K=1$ if K is the target class label for a, and zero elsewhere [51].

The general ARTMAP learning algorithm is as follow:

1. Initialization
   - All the F2 nodes are uncommitted, all weight values $\mathbf{w_{ij}}$ are initialized to 1 and all weight values $\mathbf{w_{jk}^{ab}}$ are set to 0.
   - An F2 node becomes committed when it is selected to code an input vector a , and is then linked to an F^{ab} node.
- Input pattern coding
   - Complement Coding (Normalization)
   - Training pair **(a , t)**

$$A = (a, a^c) = (a_1 , a_2 , \dots , a_m; a_1^c , a_2^c , \dots , a_m^c) \qquad (14)$$

   - The vigilance parameter is reset to its baseline value**.**

3. Prototype selection
   - F2 Activation function $T_j (A) = \frac{| A \wedge wj |}{\propto + |wj|}$ (15)
   - Greatest activation value $J = argmax \{T_j : j = 1,2,\dots,N\}$ (16)
   - Vigilance test $\frac{| A \wedge wj |}{|A|} = \frac{| A \wedge wj |}{M} \geq \rho$ (17)
   - If the test is passed, then node J remains active and resonance is said to occur.
   - If not the network inhibits the active F2, presents new training pair (a,t) or goes to step5.

4. Class prediction
   - Pattern t is fed directly to the map field F^{ab}
   - The F2 category y learns to activate the map field via associative weights W^{ab} .

$$y^{ab} = \left(y_1^{ab} , y_2^{ab} , \dots , y_L^{ab}\right) = t \wedge w_j^{ab} \qquad (18)$$

$$K = argmax \{y_k^{ab} : k = 1,2,\dots,L\} \qquad (19)$$

- Incorrect class prediction : Match tracking

$$\rho = \frac{|A \wedge wj|}{M} + \varepsilon \qquad (20)$$

5. Learning
   - Learning input a involves updating prototype vector W_J
   - if J corresponds to a newly-committed node, creating an associative link to F^{ab}

The prototype vector of F2 node J is updated according to:

$$W_J' = \beta (A \wedge wj) + (1 - \beta) wj \quad (21)$$

- Slow learning $0 < \beta < 1$ (21)
- Fast learning $\beta = 1$ (22)
- Go to Step 2

3.5.3 K-nearest Neighbor (KNN) as classifier

The nearest neighbor classification rule assigns a pattern, which is of unknown classification, to the class with the nearest neighbor. This idea has been extended to k-NN, where this classification algorithm predicts the category of the test sample on the basis of *k* training samples, which are the nearest neighbors to the test sample, and then classifies the test sample to the category that has the highest category probability. Suppose that *j* is the number of training categories, as *c1*, and the sum of the training samples is *N*. Class *X* is the same feature vector as in all the training samples. When *di* is one of the neighbors in the training set, $y(d_i, c_j) \in \{0,1\}$ indicates whether *di* belongs to class *cj*, and *Sim(X, di)* is the similarity function for X and *di*. The probability density function *P(X, cj)* for the feature data *X*, given class *cj*, can then be written as Equation (23).

$Sim\ (X, d_i)$ can be calculated with the Euclidean distance, city block, correlation, cosine, and hamming methods. In this study, the Euclidean distance method was selected because it is often used in EMG-based systems as the distance metric. The k-value is a user-defined constant number of neighbor group elements. An unlabeled vector is classified by assignment of the label that occurs most frequently among the k training samples nearest that query point. If k is significantly large, then the large classes will outperform the small ones. By contrast, the advantages of the k-NN algorithm will not be evident if k is significantly small [19]. Based on this result and on the survey conducted by Kim et al. [21] on the best k-value in terms of classification accuracy, the k-value was initially fixed at 5; it had the highest average recognition rate and the lowest standard deviation.

3.5.4 Linear Discriminant Analysis (LDA) as classifier

This study will use LDA, which is a well-known and easy to implement linear classifier, as explained in Section 3.4.2. The distance for LDA used in this thesis is the default Euclidian distance. Moreover, based on information on the cross validation in [49] a threefold cross validation was used for learning ARTMAP networks, LDA, and the k-NN classifier because the data set is large enough. The least possible computational time is also used.

4. RESULT AND DISCUSSION

For developing ART-based, LDA and KNN classifiers, the feature vectors are extracted by using proposed multi-feature from each EMG signal frame (10000 distinct samples) as described in Section 3.3 and shown in Figure 6. As a result we produced 2500 feature vectors (5 movements) for each EMG channel.. Then 1700 EMG signal patterns were randomly taken for training the neural network, LDA and KNN. The remaining 800 signal patterns were kept aside and used for testing the validity of the developed models. The class distribution of the samples in the training and testing data set is summarized in Table 2.

4.1. Evaluating redundancy of EMG features: Fuzzy C-mean clustering and scatter plot

The purpose here is to test the capability of the features in separating data into natural clusters. Therefore, how distinct the data will be after going through each feature extraction method will be analyzed by examination of the scatter plots. As a modification for FCM, the number of clusters is set to 5 (number of movements), and the data of 2 channels, namely, FCU and ECR, for one sample subject from data set#1 are considered. The result will be the comparison of single features—mean absolute value (MAV), zero crossings (ZC), slope sign changes (SSC), waveform lengths (WL), root mean square (RMS), and mean frequency (MNF) scatter plots along with the proposed multi-feature and Hudgins' multi-feature [14]—as the most effective and employed multi-features in MCS prosthetics. Figures 10 to 14 show the results of the FCM employed in each feature method. These features can be categorized into groups based on single features, similarities in scatter plots, as shown in Figures 10 to 12, and class separability.

- Figure 10 shows that RMS slightly outperforms MAV and WL in being discriminative; thus, RMS is the best single feature among all the six single features.
- ZC and SSC are a part of the second group (Figure 11), which also has the same technique in separating classes and shows good performance as a single feature but is not as discriminative as those in the first group. SSC is a better discriminator than ZC.

- The third group consists of MNF only, which is a poor single feature extractor. Its scatter plot (Figure 12) indicates that it has the least discrimination performance as long as it is not combined with other features.

With the discrimination performance of multi-features and the scatter plot observation in Figures 13 and 14 considered, the main discussion focuses on how separable and distinct can the proposed multi-feature (consisting of MAV, ZC, WL, SSC, RMS, and MNF) perform versus Hudgins' multi-feature (consisting of MAV, ZC, WL, and SSC) [42].

Initially, both feature groups may be concluded to have almost the same class separability and distinction. Further assessment, with focus on the border of class#1, class#2, and class#3, clearly indicates that the proposed multi-feature outperforms the Hudgins' multi-feature in the case of discriminative patterns between class#1 and class#3. In the proposed multi-feature (Figure 14), the two classes are separate from each other. By contrast, Figure 12 shows that the two classes overlap for Hudgins' multi-feature. Moreover, Hudgins' multi-feature had an error in discriminating class#3, whereas the other single feature methods and the proposed multi-feature method discriminate it in approximately the same neighborhood. Hudgins' multi-features clustered it near class#1, which resulted in an error. Both clustering and scatter plot can therefore be used as visual methods to evaluate feature performance and indicate the superiority of the multi-feature consisting of MAV, ZC, SSC, WL, RMS, and MNF over Hudgins' multi-feature. For further investigation and for an efficient evaluation, these features should be employed in a classification process. The classification accuracy should then be compared.

4.2. Evaluating performance of EMG features: LDA classification

Presented in this section is the outcome of the LDA classifier for the 4 channels of EMG data, 5 movement classes, and for all 12 subjects of data set#2, including the evaluation of the different features.

1 - Proposed multi-feature: MAV, ZC, WL, SSC, RMS, and MNF, as discussed in the methodology section and compared with the two best known and used multi-features.

2 - Hudgins's multi-feature: MAV, ZC, WL, and SSC [14, 42].

3 - Du's multi-feature: integrated EMG (IEMG), variance (VAR), WL, ZC, SSC, and Willison amplitude [52].

Regarding the single features, Table 3 and Figure 15 (in terms of classification performance) show that the result agrees with the feature comparison done in the previous FCM evaluation. The features are again categorized into groups as follows.

- RMS, WL, and MAV are a part of the first group, which has the best average classification accuracy among all features at 65.28%, 63.29%, and 56.54%, respectively. This result means that they are more capable of extracting features for movement classification than other single features do.
- ZC and SSC are a part of the second group, which also has the same poor manner of separating classes. SSC (24.29% ± 4.59%) has a better classification performance than ZC (14.35% ± 4.50%).
- The third group consists of MNF only, which is a poor single feature extractor. The classification accuracy of MNF with the use of LDA as classifier is as low as 11.39% ± 2.12%.

Table 3 and Figure 15 show and consider the classification performance of multi-feature. Based on LDA classification accuracy results, the conclusion is that the proposed multi-feature, which has an average accuracy of 82.51% ± 5.56% over all the 12 subjects, outperforms Du's multi-feature (76.46% ± 4.09%) and Hudgins' multi-feature (75.84% ± 3.23%) by at least 6% average classification accuracy. Therefore, based on the FCM scatter plots and LDA classification evaluation, the proposed multi-feature consisting of MAV, ZC, WL, SSC, RMS, and MNF can be used as an optimal choice for feature extraction because it has acceptable class separability, redundancy, and classification accuracy compared with those of Hudgins and Du.

4.3. Classification results and discussion:

Presented in this section is the classification result comparison of the main data set (data set 2) that considers 12 subjects and 4 EMG channels to classify 5 different hand movements. The comparison has been made among four different ART-based network classifiers, including the Best-ART approach among them and LDA (as the best known one in terms of simplicity and accuracy in learning classifiers) and k-NN (as one of the most simple and applicable statistical classification approaches).

Based on classification performance, as shown in Table 4 and Figure 16, and in terms of classification accuracy, ART-based classifiers outperform k-NN and LDA. By contrast, Best-ART with 89.09% ± 3.27% has the best accuracy among all ART-based methods and is superior to those of k-NN (83.98% ± 3.70%) and LDA (82.52% ± 5.81%). However, Lock et al. [50] explained that a high classification accuracy can result in good performance if the classifier also has good performance in terms of computation time parameters. Further classifier evaluation indicates that this outcome is the result of computational time comparison, including training time (TT), classification time (CT), and elapsed time (ET) between ART-based classifiers and k-NN and LDA. Moreover, ET is the time it takes for the CPU to run the entire process of classification of hand movements, from initialization to the end of classification.

Tabel 5 and Figures 17a and 17b show the average TT, CT, and ET results over all 12 subjects included in the Southampton data set; the first two are in ms and the last one is in s. With the TT among the ART-based classifiers considered, all subjects need the same time for training features, except for fuzzy-ARTMAP, which takes a little longer (94.26 ms) to train. However, comparison of Best-ART (as the best ART method) with k-NN and LDA shows that the former outperforms the latter two. Best-ART takes 73.41 ms, which is approximately half of the TT needed for k-NN and LDA.
Regarding the CT, the trend for ART-based classifiers is almost the same as that of the TT, except for dARTMAP, which takes 43.5 ms less to classify than the others do.

The difference between Best-ART and k-NN and LDA is highly significant, with Best-ART considered superior. Best-ART takes an average of 49.57 ms to classify the correct movements, and this is approximately one-fifth of k-NN (230.91 ms) and one-seventh of LDA (344.2 ms).
Finally, when it comes to the average ET, ART-based classifiers show better classification performance in a significantly shorter time than LDA and k-NN do, as shown in Figure 15b. ART-based classifiers only take approximately 4 s to perform the entire process of hand movement classification, whereas k-NN executes it in 6.58 s, and LDA even takes longer with an average time of 7.92 s.

4.4 Classifiers' Statistical analysis using ANOVA.

As the final step of classifier evaluation, a statistical analysis test, one-way ANOVA, and post hoc comparison test were conducted to investigate the difference in classification accuracy of the proposed algorithms from a statistical point of view. These tests were also conducted to check the significance of classifier performance, namely, that of Best-ART over k-NN and LDA. Regarding data set 2, a significant difference in classification accuracy exists among the three classifiers at 0.05 significance level, [F (2, 33) 11.473, p = .0002]. Post hoc comparisons using the Tukey HSD test indicated that the Best-ART (M =89.075, SD=3.27) significantly performed a more accurate classification than KNN (M=83.98, SD=3.70), p=0.0002. Moreover, Best-ART had a significantly higher classification accuracy than LDA (M=82.516, SD=5.81), p=0.003. However, no significant difference existed in the classification accuracy between LDA (M=82.516, SD=5.813) and KNN (M=83.98, SD=3.70), p=0.676.

5. CONCLUSION

The main objective of this research was to propose a simple pattern recognition approach in efficiently classifying hand movements from EMG signals. A new combination of time-domain features, namely, MAV, ZC, SSC, WL, RMS, and MNF, was investigated and evaluated. The result indicated the good performance of this research multi-feature in terms of both class separability (comparing scatter plots) and LDA classification accuracy. The proposed method has an accuracy of 82.51% against Hudgins' 75.84% and Du's 76.46%.

This optimal multi-feature was used in a pattern recognition system in which five distinct hand movements were classified with a hybrid ART-based neural network classification approach. A second evaluation process was utilized on classification methods for the main data set and the additional data set. Regarding the classification accuracy of the main data set (Ahmad 2009), single session results obtained from 12 healthy subjects indicated an average accuracy of 89.09% for Best-ART, 83.98% for k-NN, and 82.52% for LDA. By contrast, the classification accuracy obtained from four healthy subjects in the additional data set (Theodoridis 28/07/11) is 95.7% for Best-ART, 89.42% for k-NN, and 88.86% for LDA. This result clearly indicated the performance superiority of the ART-based classifier over the other two. Further investigation was conducted through computation time evaluation of the proposed ART-based methods, LDA, and k-NN. Regarding TT (ms), CT (ms), and ET (s), the evaluation on both data sets indicated the significantly less computation time of the ART-based methods compared with LDA and k-NN.

The evaluation results demonstrated the superiority of the proposed pattern recognition approach for hand movement classification in terms of feature redundancy, feature extraction accuracy, movement classification accuracy, computation time, and statistical significance. The proposed MCS in this study can be widely used and applied as a potential control approach and as foundation for designing an effective and affordable prosthetic hand in real-time applications.

REFRENCES

[1] S. Allin, E. Eckel, H. Markham, and B. R. Brewer, "Recent trends in the development and evaluation of assistive robotic manipulation devices," *Physical medicine and rehabilitation clinics of North America,* vol. 21, pp. 59-77, 2010.

[2] P. Zhou, B. Lock, and T. A. Kuiken, "Real time ECG artifact removal for myoelectric prosthesis control," *Physiological measurement,* vol. 28, p. 397, 2007.

[3] C. Castellini and P. van der Smagt, "Surface EMG in advanced hand prosthetics," *Biological cybernetics,* vol. 100, pp. 35-47, 2009.

[4] H. Liu and L. Yu, "Toward integrating feature selection algorithms for classification and clustering," *Knowledge and Data Engineering, IEEE Transactions on,* vol. 17, pp. 491-502, 2005.

[5] P. J. Kyberd, A. Murgia, M. Gasson, T. Tjerks, C. Metcalf, P. H. Chappell*, et al.*, "Case studies to demonstrate the range of applications of the Southampton Hand Assessment Procedure," *The British Journal of Occupational Therapy,* vol. 72, pp. 212-218, 2009.

[6] M. Asghari Oskoei and H. Hu, "Myoelectric control systems—A survey," *Biomedical Signal Processing and Control,* vol. 2, pp. 275-294, 2007.

[7] C. Pylatiuk, S. Schulz, and L. Döderlein, "Results of an Internet survey of myoelectric prosthetic hand users," *Prosthetics and orthotics international,* vol. 31, pp. 362-370, 2007.

[8] P. J. Kyberd and P. Chappell, "The Southampton Hand: an intelligent myoelectric prosthesis," *Journal of rehabilitation Research and Development,* vol. 31, p. 326, 1994.

[9] A. B. Ajiboye and R. F. Weir, "A heuristic fuzzy logic approach to EMG pattern recognition for multifunctional prosthesis control," *Neural Systems and Rehabilitation Engineering, IEEE Transactions on,* vol. 13, pp. 280-291, 2005.

[10] R. N. Khushaba, A. Al-Ani, and A. Al-Jumaily, "Orthogonal fuzzy neighborhood discriminant analysis for multifunction myoelectric hand control," *Biomedical Engineering, IEEE Transactions on,* vol. 57, pp. 1410-1419, 2010.

[11] R. N. Khushaba, A. Al-Jumaily, and A. Al-Ani, "Novel feature extraction method based on fuzzy entropy and wavelet packet transform for myoelectric control," in *Communications and Information Technologies, 2007. ISCIT'07. International Symposium on*, 2007, pp. 352-357.

[12] H. Jahani Fariman, S. A. Ahmad, M. Hamiruce Marhaban, M. Ali Jan Ghasab, and P. H. Chappell, "Simple and Computationally Efficient Movement Classification Approach for EMG-controlled Prosthetic Hand: ANFIS vs. Artificial Neural Network," *Intelligent Automation & Soft Computing,* pp. 1-15, 2015.

[13] M. A. J. Ghasab, S. Khamis, F. Mohammad, and H. J. Fariman, "Feature decision-making ant colony optimization system for an automated recognition of plant species," *Expert Systems with Applications,* vol. 42, pp. 2361-2370, 2015.

[14] A. Phinyomark, P. Phukpattaranont, and C. Limsakul, "Feature reduction and selection for EMG signal classification," *Expert Systems with Applications,* vol. 39, pp. 7420-7431, 2012.

[15] L. Hargrove, K. Englehart, and B. Hudgins, "The effect of electrode displacements on pattern recognition based myoelectric control," in *Engineering in Medicine and Biology Society, 2006. EMBS'06. 28th Annual International Conference of the IEEE*, 2006, pp. 2203-2206.

[16] Y. Losier, K. Englehart, and B. Hudgins, "A control system for a powered prosthesis using positional and myoelectric inputs from the shoulder complex," in *Conference proceedings:... Annual International Conference of the IEEE Engineering in Medicine and Biology Society. IEEE Engineering in Medicine and Biology Society. Conference*, 2007, p. 6138.

[17] L. J. Hargrove, K. Englehart, and B. Hudgins, "A comparison of surface and intramuscular myoelectric signal classification," *Biomedical Engineering, IEEE Transactions on,* vol. 54, pp. 847-853, 2007.

[18] X. Hu, P. Yu, Q. Yu, W. Liu, and J. Qin, "Classification of surface EMG signal based on energy spectra change," in *BioMedical Engineering and Informatics, 2008. BMEI 2008. International Conference on*, 2008, pp. 375-379.

[19] S. Rasheed, D. Stashuk, and M. Kamel, "Adaptive fuzzy< i> k</i>-NN classifier for EMG signal decomposition," *Medical engineering & physics,* vol. 28, pp. 694-709, 2006.

[20] S. Rasheed, D. Stashuk, and M. Kamel, "A software package for interactive motor unit potential classification using fuzzy< i> k</i>-NN classifier," *Computer methods and programs in biomedicine,* vol. 89, pp. 56-71, 2008.

[21] K. S. Kim, H. H. Choi, C. S. Moon, and C. W. Mun, "Comparison of< i> k</i>-nearest neighbor, quadratic discriminant and linear discriminant analysis in classification of electromyogram signals based on the wrist-motion directions," *Current applied physics,* vol. 11, pp. 740-745, 2011.

[22] S. Aditya and D. Tibarewala, "Comparing ANN, LDA, QDA, KNN and SVM algorithms in classifying relaxed and stressful mental state from two–channel prefrontal EEG data," *International Journal of Artificial Intelligence and Soft Computing,* vol. 3, pp. 143-164, 2012.

[23] A. Phinyomark, F. Quaine, S. Charbonnier, C. Serviere, F. Tarpin-Bernard, and Y. Laurillau, "EMG feature evaluation for improving myoelectric pattern recognition robustness," *Expert Systems with Applications,* vol. 40, pp. 4832-4840, 2013.

[24] G. A. Carpenter, S. Grossberg, and J. H. Reynolds, "ARTMAP: Supervised real-time learning and classification of nonstationary data by a self-organizing neural network," *Neural networks,* vol. 4, pp. 565-588, 1991.

[25] S. J. Verzi, G. L. Heileman, M. Georgiopoulos, and M. J. Healy, "Hierarchical ARTMAP," in *Neural Networks, 2000. IJCNN 2000, Proceedings of the IEEE-INNS-ENNS International Joint Conference on*, 2000, pp. 41-46.

[26] H. Xu, "Mahalanobis distance based ARTMAP networks," San Diego State University, 2003.

[27] H. Xu and M. Vuskovic, "Mahalanobis distance-based artmap network," in *Neural Networks, 2004. Proceedings. 2004 IEEE International Joint Conference on*, 2004, pp. 2353-2359.

[28] G. Carpenter, S. Grossberg, and K. Iizuka, "Comparative performance measures of fuzzy ARTMAP, learned vector quantization, and back propagation for handwritten character recognition," in *Neural Networks, 1992. IJCNN., International Joint Conference on*, 1992, pp. 794-799.

[29] G. A. Carpenter, B. L. Milenova, and B. W. Noeske, "Distributed ARTMAP: a neural network for fast distributed supervised learning," *Neural networks,* vol. 11, pp. 793-813, 1998.

[30] A. Nachev, S. Hill, C. Barry, and B. Stoyanov, "Fuzzy, distributed, instance counting, and default artmap neural networks for financial diagnosis," *International Journal of Information Technology & Decision Making,* vol. 9, pp. 959-978, 2010.

[31] G. A. Carpenter, S. Grossberg, N. Markuzon, J. H. Reynolds, and D. B. Rosen, "Fuzzy ARTMAP: A neural network architecture for incremental supervised learning of analog multidimensional maps," *Neural Networks, IEEE Transactions on,* vol. 3, pp. 698-713, 1992.

[32] E. Llobet, J. Brezmes, R. Ionescu, X. Vilanova, S. Al-Khalifa, J. Gardner*, et al.*, "Wavelet transform and fuzzy ARTMAP-based pattern recognition for fast gas identification using a micro-hotplate gas sensor," *Sensors and Actuators B: Chemical,* vol. 83, pp. 238-244, 2002.

[33] G. A. Carpenter and N. Markuzon, "ARTMAP-IC and medical diagnosis: Instance counting and inconsistent cases," *Neural Networks,* vol. 11, pp. 323-336, 1998.

[34] G. A. Carpenter and W. D. Ross, "ART-EMAP: A neural network architecture for object recognition by evidence accumulation," *Neural Networks, IEEE Transactions on,* vol. 6, pp. 805-818, 1995.

[35] S. J. Verzi, G. L. Heileman, M. Georgiopoulus, and M. J. Healy, "Rademacher penalization applied to Fuzzy ARTMAP and Boosted ARTMAP," in *Neural Networks, 2001. Proceedings. IJCNN'01. International Joint Conference on*, 2001, pp. 1191-1196.

[36] H. J. Hermens, B. Freriks, R. Merletti, D. Stegeman, J. Blok, G. Rau*, et al.*, "European recommendations for surface electromyography," *Roessingh Research and Development, Enschede,* 1999.

[37] T. Theodoridis, "EMG Physical Action DataSet," ed. School of Computer Science and Electronic Engineering, University of Essex, 28/07/11.

[38] S. A. Ahmad, "Moving approximate entropy and its application to the electromyographic control of an artificial hand," University of Southampton, 2009.

[39] K. Englehart and B. Hudgins, "A robust, real-time control scheme for multifunction myoelectric control," *Biomedical Engineering, IEEE Transactions on,* vol. 50, pp. 848-854, 2003.

[40] S. Du and M. Vuskovic, "Temporal vs. spectral approach to feature extraction from prehensile EMG signals," in *Information Reuse and Integration, 2004. IRI 2004. Proceedings of the 2004 IEEE International Conference on*, 2004, pp. 344-350.

[41] M. A. Oskoei and H. Hu, "Support vector machine-based classification scheme for myoelectric control applied to upper limb," *Biomedical Engineering, IEEE Transactions on,* vol. 55, pp. 1956-1965, 2008.

[42] B. Hudgins, P. Parker, and R. N. Scott, "A new strategy for multifunction myoelectric control," *Biomedical Engineering, IEEE Transactions on,* vol. 40, pp. 82-94, 1993.

[43] M. Zardoshti-Kermani, B. C. Wheeler, K. Badie, and R. M. Hashemi, "EMG feature evaluation for movement control of upper extremity prostheses," *Rehabilitation Engineering, IEEE Transactions on,* vol. 3, pp. 324-333, 1995.

[44] R. Boostani and M. H. Moradi, "Evaluation of the forearm EMG signal features for the control of a prosthetic hand," *Physiological measurement,* vol. 24, p. 309, 2003.

[45] L. Philipson, "The electromyographic signal used for control of upper extremity prostheses and for quantification of motor blockade during epidural anaesthesia," Linköping, 1987.

[46] B. Karlik, M. Osman Tokhi, and M. Alci, "A fuzzy clustering neural network architecture for multifunction upper-limb prosthesis," *Biomedical Engineering, IEEE Transactions on,* vol. 50, pp. 1255-1261, 2003.

[47] Y.-C. Du, C.-H. Lin, L.-Y. Shyu, and T. Chen, "Portable hand motion classifier for multi-channel surface electromyography recognition using grey relational analysis," *Expert Systems with Applications,* vol. 37, pp. 4283-4291, 2010.
[48] G. A. Carpenter and S. Grossberg, "A self-organizing neural network for supervised learning, recognition, and prediction," *Communications Magazine, IEEE,* vol. 30, pp. 38-49, 1992.
[49] U. M. Braga-Neto and E. R. Dougherty, "Is cross-validation valid for small-sample microarray classification?," *Bioinformatics,* vol. 20, pp. 374-380, 2004.
[50] B. Lock, K. Englehart, and B. Hudgins, "Real-time myoelectric control in a virtual environment to relate usability vs. accuracy," 2005.
[51] E. Granger, M. A. Rubin, S. Grossberg, and P. Lavoie, "A what-and-where fusion neural network for recognition and tracking of multiple radar emitters," *Neural Networks,* vol. 14, pp. 325-344, 2001.
[52] S. Du, "Feature extraction for classification of prehensile electromyography patterns," San Diego State University, 2003.

Tables:

Table 1. Data acquisition and pre-processing details.

Subjects	**12** normal-limb subjects; Between 20 and 30 years old
Channels (Muscles) Shown in Figure 3.	**4** EMG channels; 1. Flexor carpi ulnaris (**FCU**) 2. Extensor carpi radialis (**ECR**) 3. Biceps brachii (**BB**) 4. Triceps brachii (**TB**)
Movements Shown in Figure 4.	**5** essential hand movements; 1. Wrist flexion/extension 2. Elbow flexion 3. Finger flexion/extension 4. Co-contraction 5. Isometric contraction
Signal recording time	Each recording: - **7** seconds - 5 to 10 muscle contractions
Signal segmentation	Each segment: - 265.5 ms - 123 ms overlapped
Sampling rate	SEMG signals were sampled at **1500 Hz**.

Table 2: Distribution of feature samples in training and testing set.

EMG Channel	Training set	Testing set	Total
Channel#1 (FCU)	1700	800	2500 (5 movements)
Channel#2 (ECU)	1700	800	2500 (5 movements)
Channel#3 (BB)	1700	800	2500 (5 movements)
Channel#4 (TB)	1700	800	2500 (5 movements)
Total	6800	3200	10000 (5 movements)

Table 3 : result of Linear Discriminant analysis (LDA) classification for evaluating different features.

		Feature	Average accuracy (12 subjects)	±SD
Surface EMG	**Overlapped Windowing**	MAV	56.54	6.29
		ZC	14.35	4.50
		WL	63.29	5.51
		SSC	24.29	4.59
		RMS	65.28	5.15
		MNF	11.39	2.12
		Hudgins' multi-feature	***75.84***	3.23
		Du's multi-feature	***76.46***	4.09
		Proposed multi-feature	***82.51***	5.56

Table 4: Classification accuracy result of all 12 subjects main dataset for 7 classifiers.

			Classifier	Average accuracy (12 subjects)	±SD
Surface EMG (Main dataset)	Overlapped Windowing	Proposed multi-feature	dARTMAP	85.84	4.80
			ART-EMAP	80.86	16.92
			ARTMAP-IC	83.71	6.58
			Fuzzy ARTMAP	85.98	6.25
			Best-ART	**89.09**	3.27
			KNN	**83.98**	3.70
			LDA	***82.52***	5.81

Table 5: Computational time comparison result for ART-based methods, LDA and KNN, averaged on all 12 subjects dataset#2.

Average time	KNN	LDA	fuzzy-ARTMAP	Best-ART	ART-EMAP	ARTMAP-IC	dARTMAP
Training (ms)	165.42	153.65	94.26	75.69	73.66	73.58	73.41
Classification (ms)	230.91	344.2	52.12	49.57	52.66	53.58	43.5
Elapsed (s)	6.58	7.92	3.77	4.05	3.88	3.84	3.85

Figure Captions:

Figure 1. Myoelectric pattern recognition prosthetic hand scheme.

Figure 2. Pattern classification methodology scheme in this paper.

Figure 3: Anatomy of 4 different muscles used in EMG dataset; modified from [23].

Figure 4: Hand Movements; (a) wrist flexion/extension, (b) elbow flexion, (c) finger flexion/extension, (d) Co-contraction and (e) Isometric contraction.

Figure 5: Overlapping windowing technique [6].

Figure 6: Example of a full segment of EMG signal consists of all 5 movements.

Figure 7: Feature extraction process.

Figure 8: Combined ART method (Best-ART) flowchart.

Figure 9: ARTMAP neural network architecture specialized for pattern classification [51].

Figure 10: Scatter plot of (a) MAV, (b) WL and (c) RMS as feature extractors for dataset#1.

Figure 11: Scatter plot of ZC (a) and SSC (b) as feature extractors for dataset#1.

Figure 12: Scatter plot of MNF as feature extractor for dataset#1.

Figure 13: Scatter plot of Hudgins's multi-feature as feature extractor for dataset#1.

Figure 14: Scatter plot of the proposed multi-feature as feature extractor for dataset#1.

Figure 15: Result of Linear Discriminant analysis (LDA) classification for evaluating different features.

Figure 16: Accuracy comparison between Best-ART method, KNN and LDA for all 12 subjects (dataset#2) and average.

Figure 17: a) Average Training Time (ms) and Classification Time (ms) for classifiers over all subjects main dataset, b) Average Elapsed Time (s) for the classifiers over all 12 subjects dataset#2.

Figures:

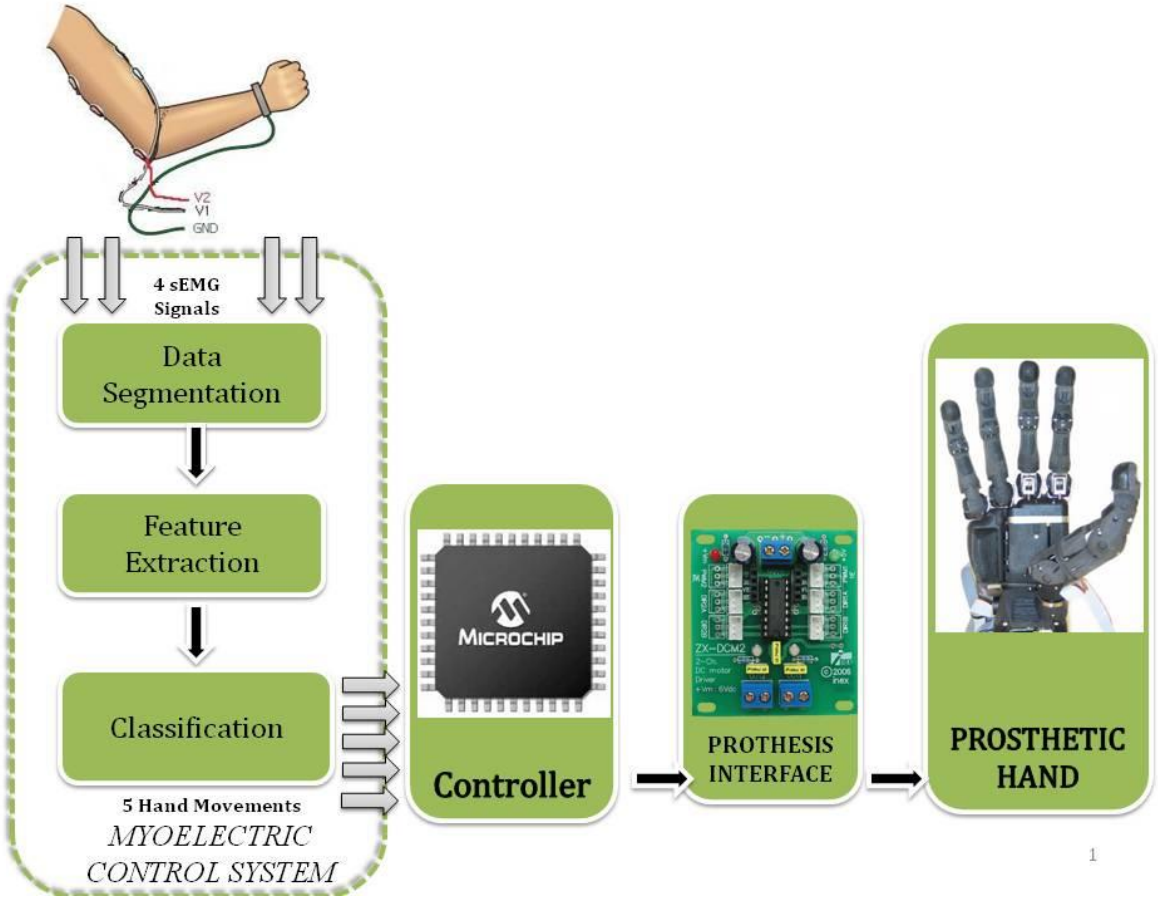

Figure 1. The scheme of myoelectric pattern recognition-based prosthetic hand.

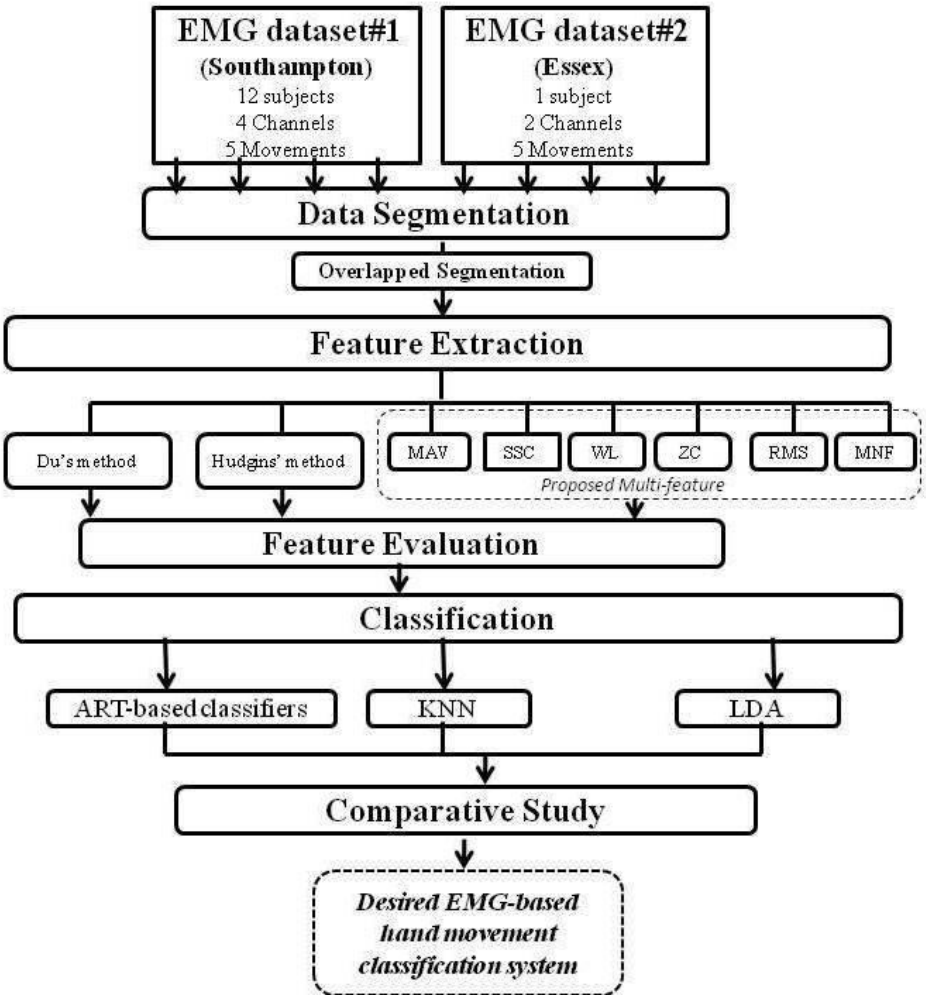

Figure 2. Pattern classification methodology scheme in this paper.

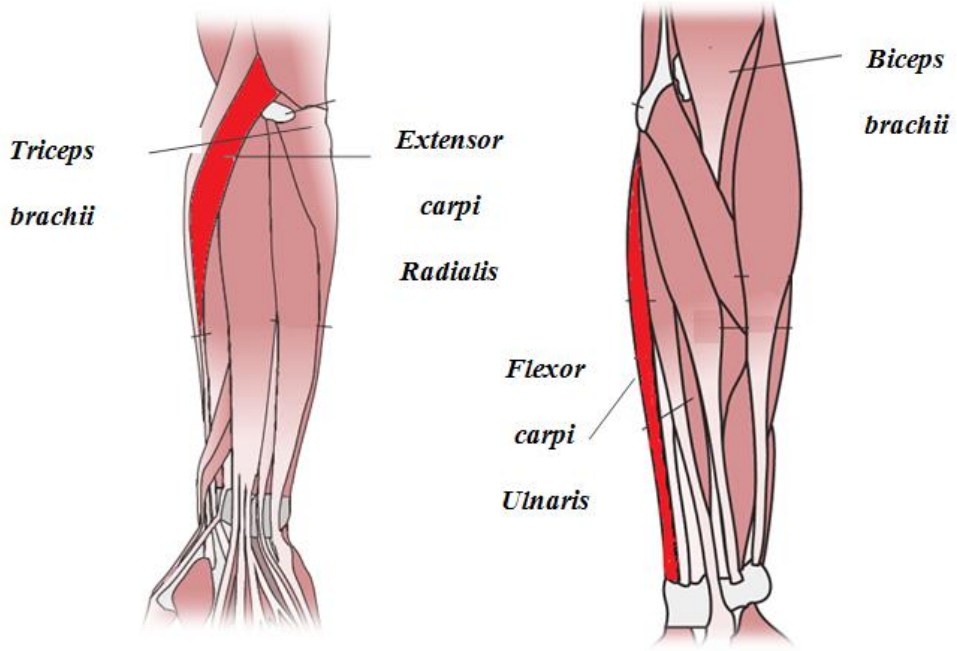

Figure 3: Anatomy of 4 different muscles used in EMG dataset; modified from [23].

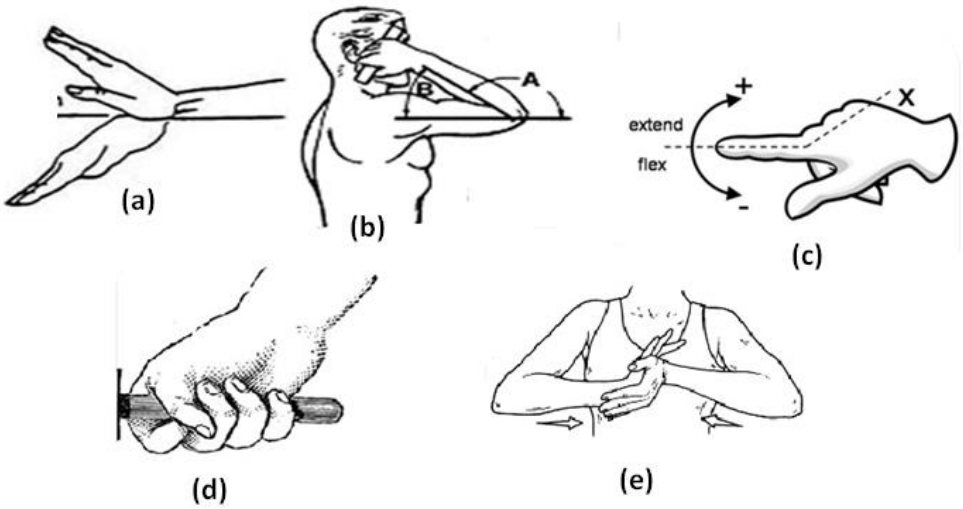

Figure 4: Hand Movements; (a) wrist flexion/extension, (b) elbow flexion, (c) finger flexion/extension, (d) Co-contraction and (e) Isometric contraction.

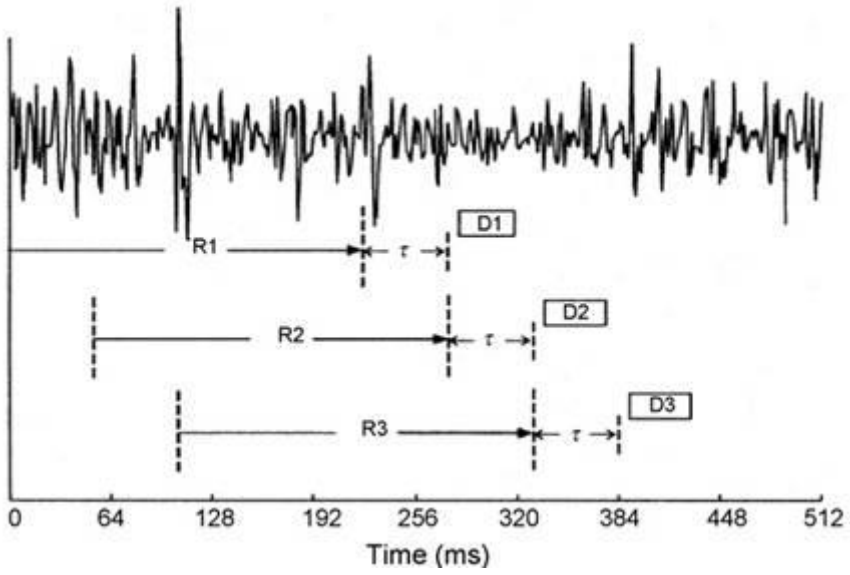

Figure 5: Overlapping windowing technique [6].

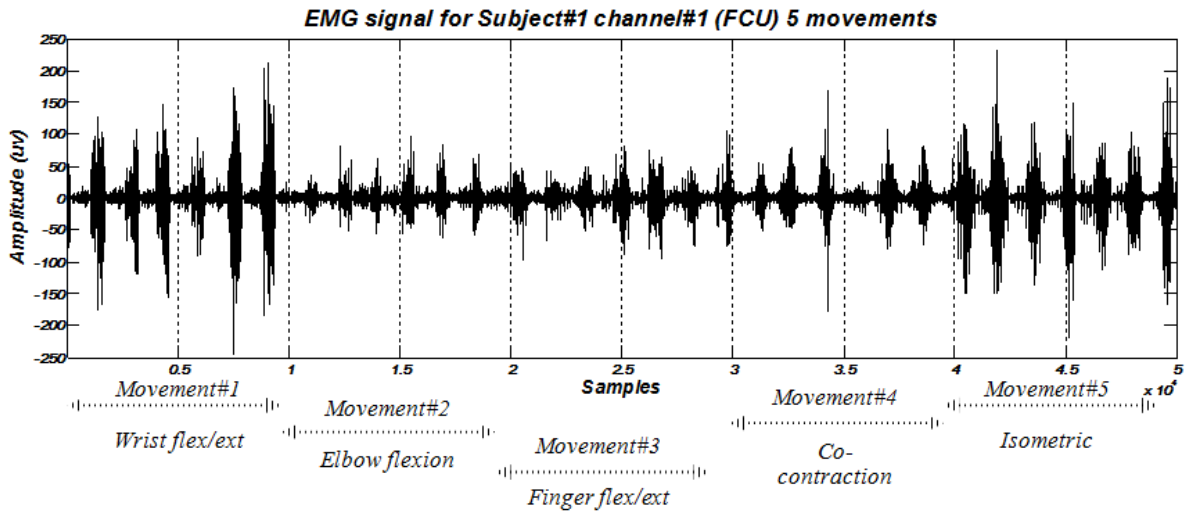

Figure 6: Example of a full segment of EMG signal consists of all 5 movements.

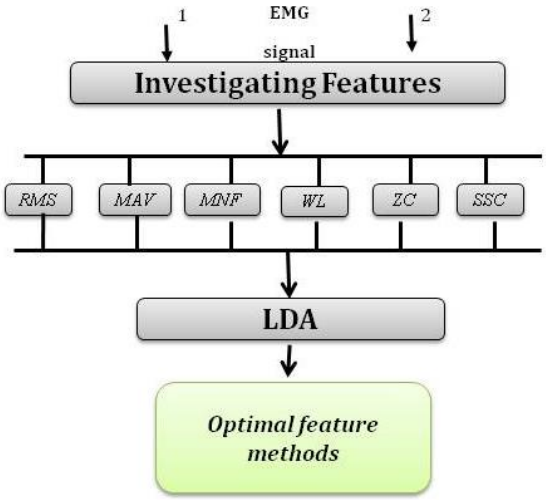

Figure 7: Feature extraction process.

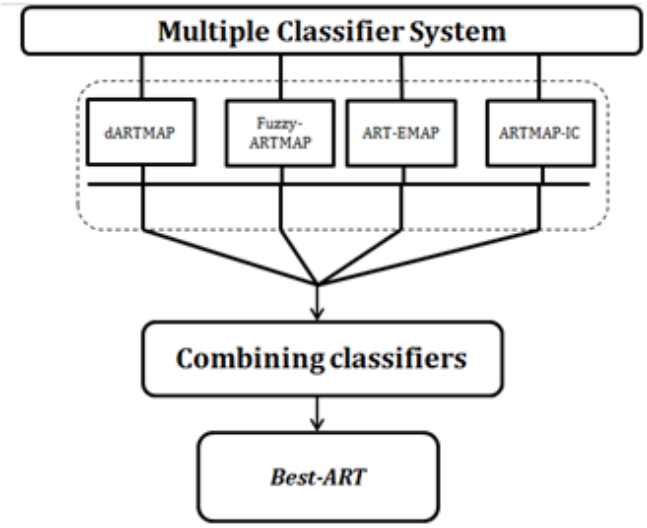

Figure 8: Combined ART method (Best-ART) flowchart.

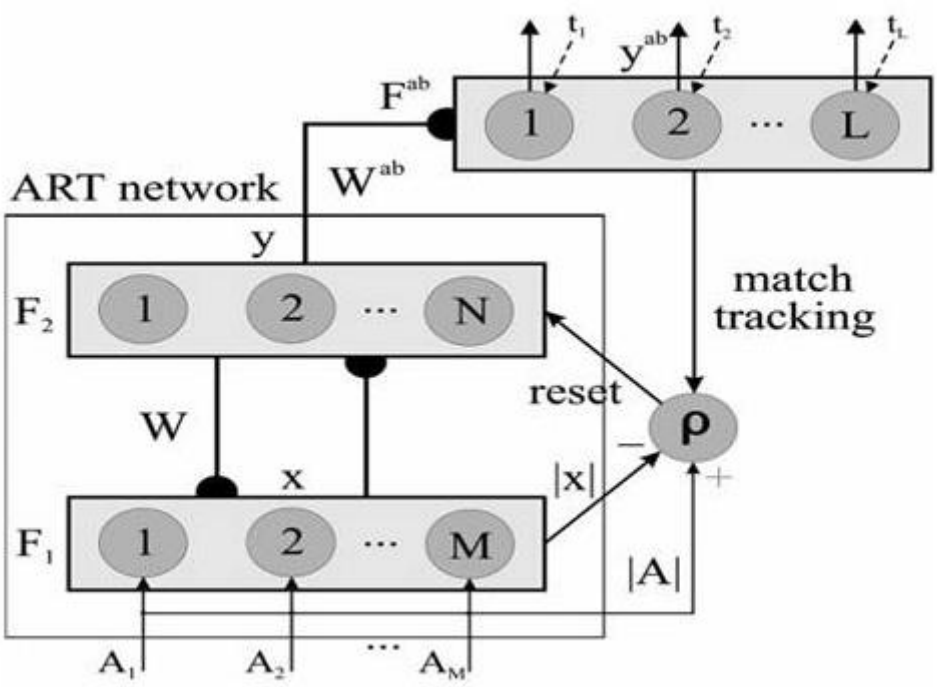

Figure 9: ARTMAP neural network architecture specialized for pattern classification [51].

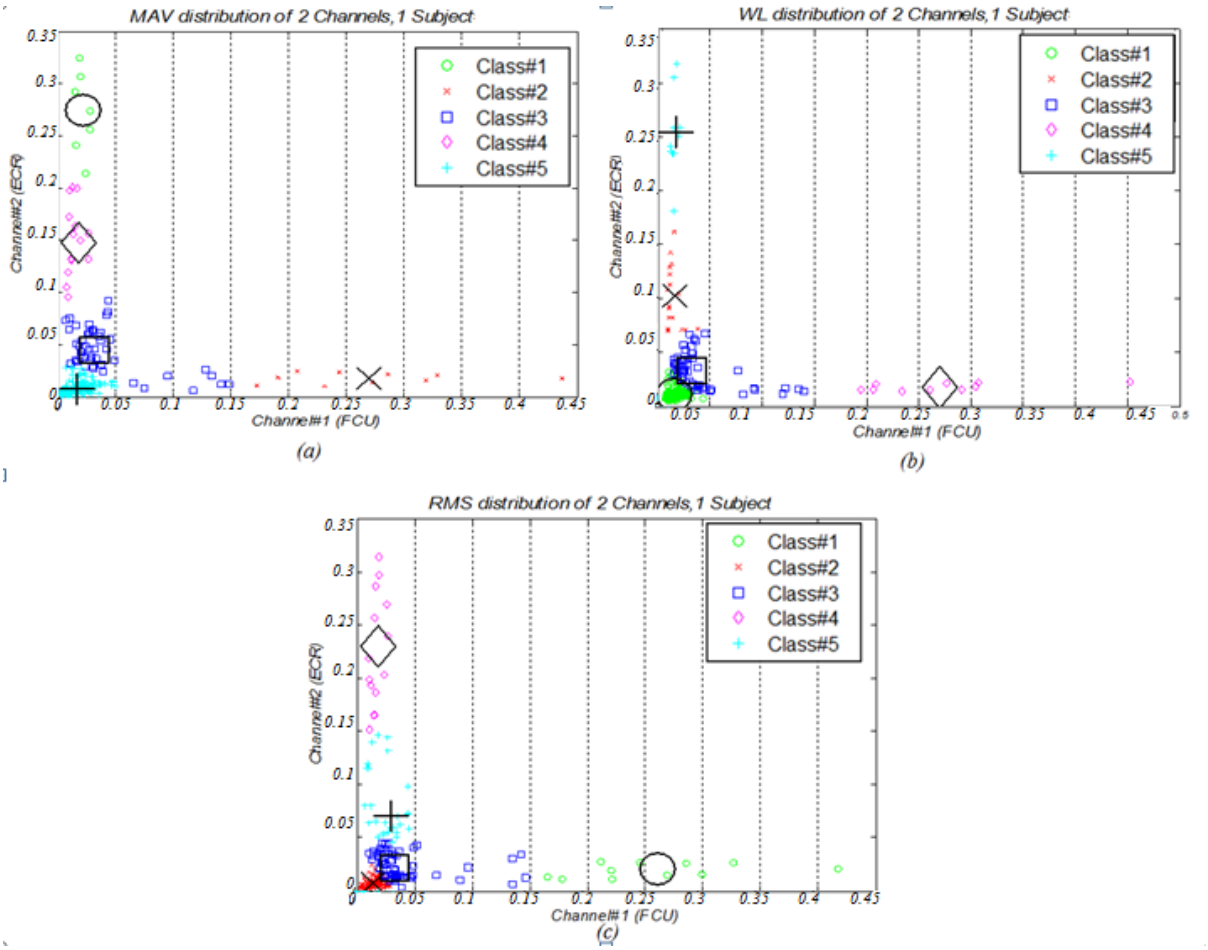

Figure 10: Scatter plot of (a) MAV, (b) WL and (c) RMS as feature extractors for dataset#1.

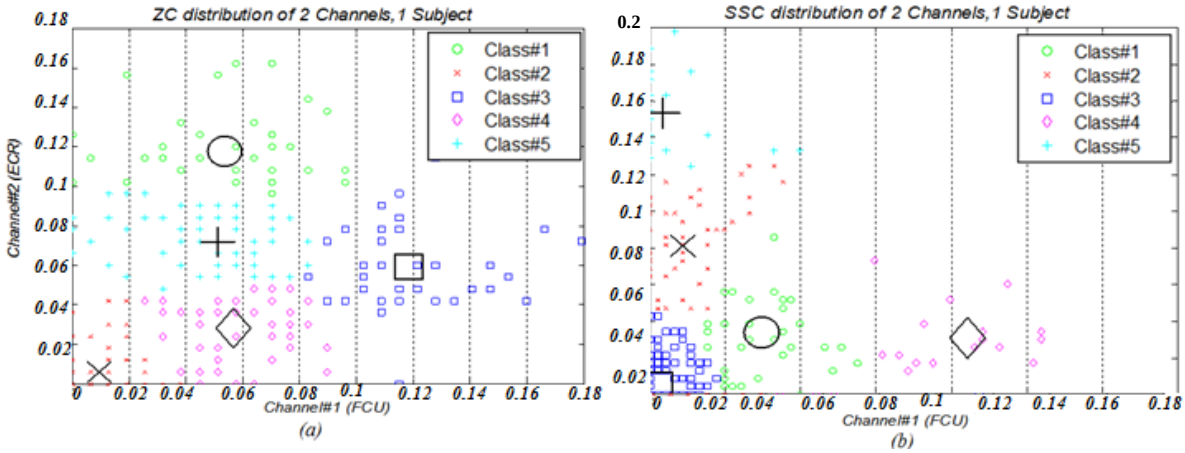

Figure 11: Scatter plot of ZC (a) and SSC (b) as feature extractors for dataset#1.

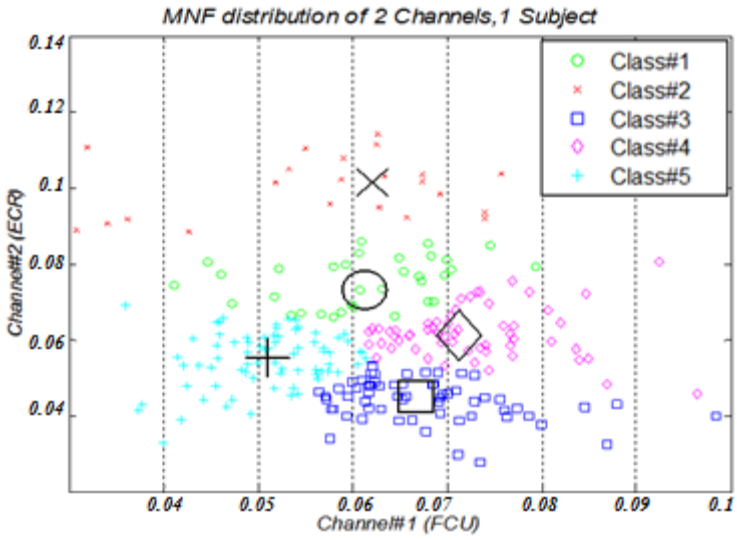

Figure 12: Scatter plot of MNF as feature extractor for dataset#1.

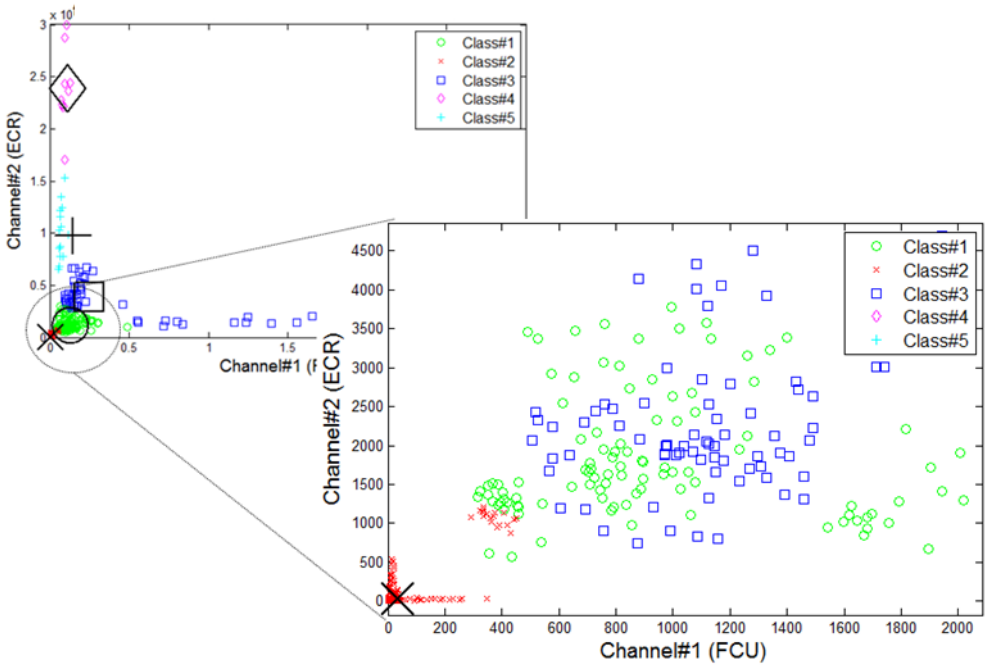

Figure 13: Scatter plot of Hudgins's multi-feature as feature extractor for dataset#1.

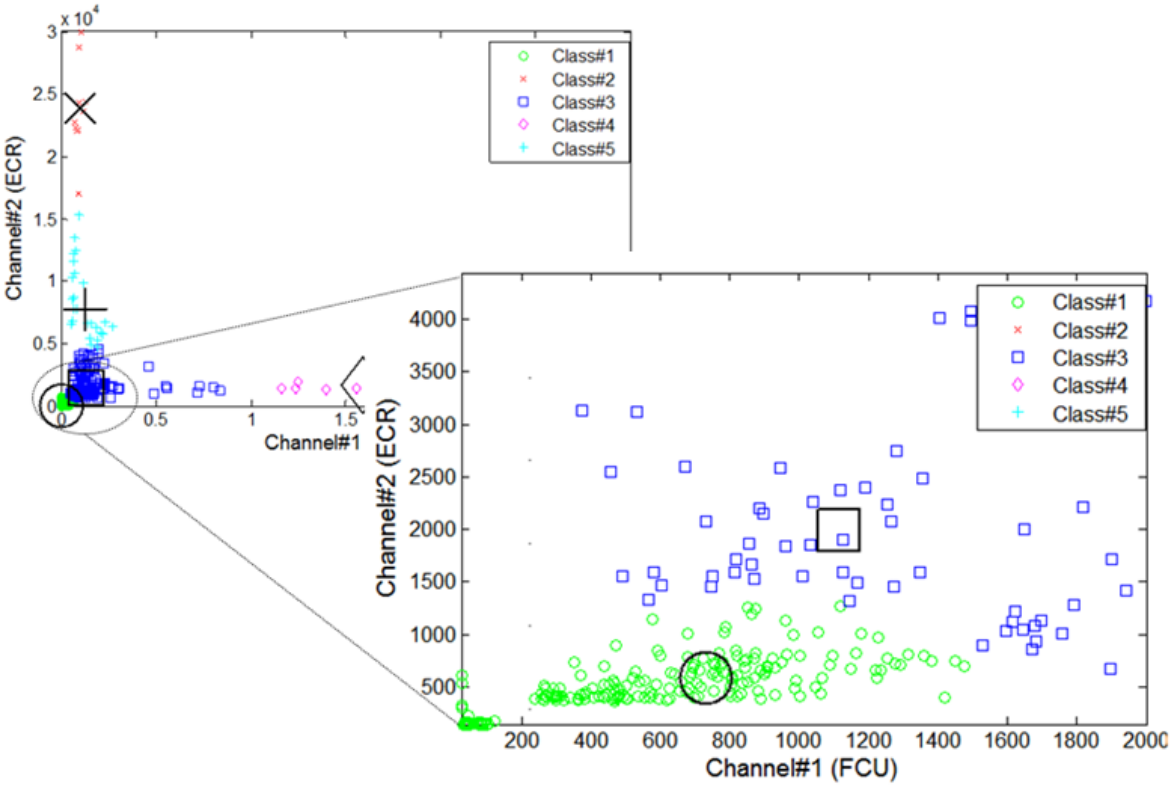

Figure 14: Scatter plot of the proposed multi-feature as feature extractor for dataset#1.

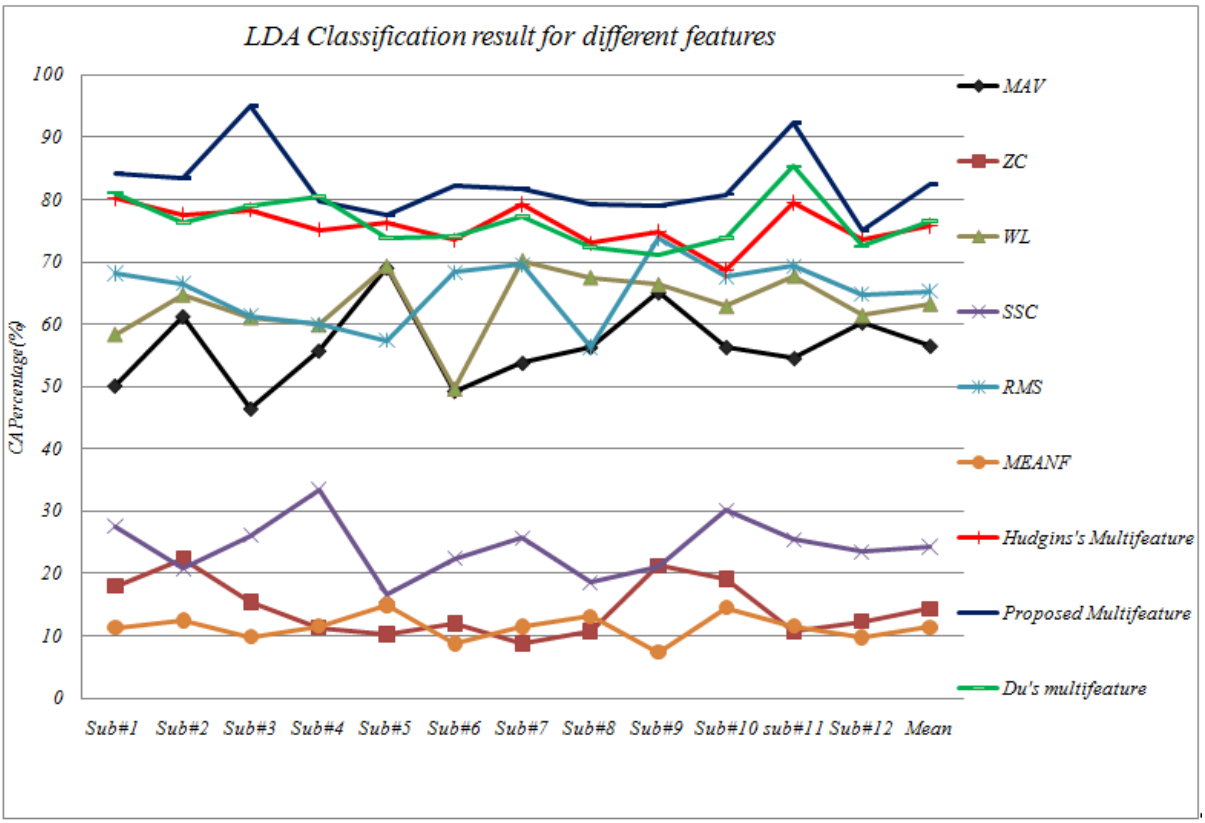

Figure 15: Result of Linear Discriminant analysis (LDA) classification for evaluating different features.

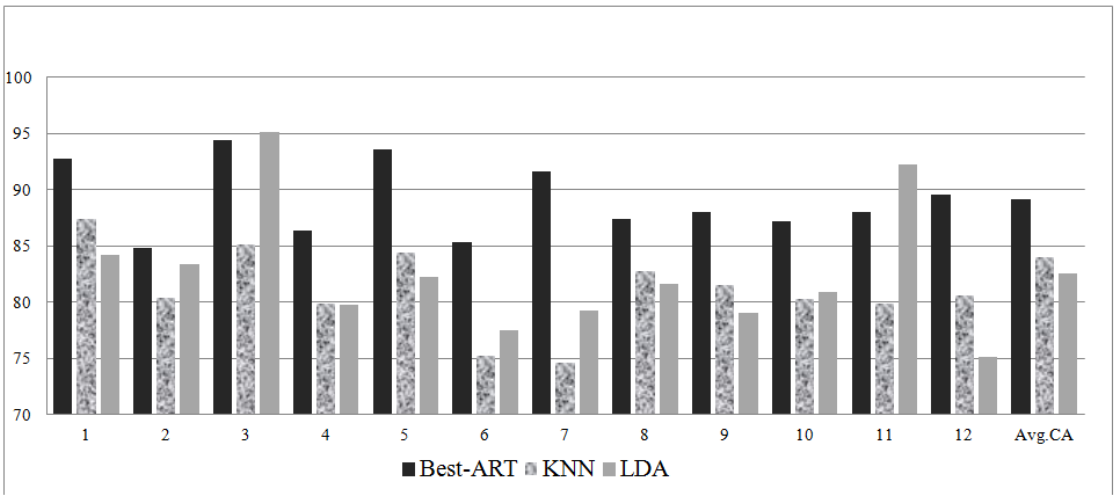

Figure 16: Accuracy comparison between Best-ART method, KNN and LDA for all 12 subjects (dataset#2) and average.

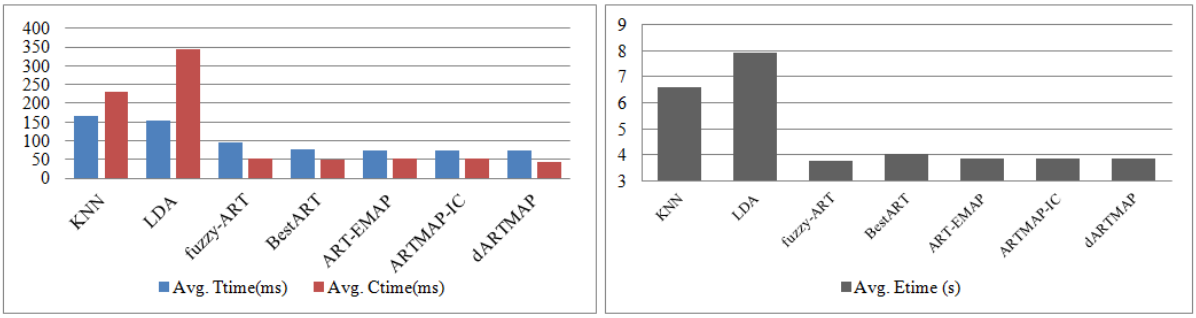

Figure 17: a) Average Training Time (ms) and Classification Time (ms) for classifiers over all subjects main dataset, b) Average Elapsed Time (s) for the classifiers over all 12 subjects dataset#2.